Climatologie 2022, 19, 5

https://doi.org/10.1051/climat/202219005

Available online :
https://climatology.edpsciences.org

Temperature inversions in France – Part B: Spatial variations

Daniel Joly [1*], Yves Richard [2]

[1] Laboratoire ThéMA, CNRS and Université Bourgogne Franche-Comté, Besançon, France

[2] Centre de Recherches de Climatologie / Biogéosciences, CNRS and Université Bourgogne Franche-Comté, Dijon, France

Résumé – **Inversions de température en France – Partie B : variations spatiales**. La base de données étudiée comprend les températures minimales et maximales quotidiennes observées sur 10 ans dans 859 paires de stations météorologiques réparties sur toute la France. Chaque paire associe une station basse et une station haute. L'influence de six prédicteurs sur l'intensité, la fréquence et la durée des inversions de température est mesurée par des régressions linéaires. Cinq prédicteurs sont tirés d'un MNT à 250 m de résolution : l'altitude, la profondeur de la vallée où sont situées les stations basses, l'amplitude du relief positif (crête, collines), le gradient de la pente des reliefs et l'amplitude altitudinale entre la station haute et la station basse. Le sixième descripteur utilisé est la distance à la mer ou à l'océan le plus proche. La topographie exerce une influence majeure dans la formation des inversions thermiques. Trois des descripteurs expliquent plus de 80 % de la variance des caractères d'inversion : la distance à la mer, la profondeur des vallées et l'amplitude altitudinale. L'altitude n'explique que 24 % de cette variance. La distribution spatiale des trois caractéristiques des inversions met en évidence plusieurs catégories qui s'inscrivent dans plusieurs échelles emboîtées. Les 859 sites peuvent être classés en trois classes relatives aux montagnes, aux zones côtières et aux plateaux. Cependant, leur répartition sur la zone étudiée ne permet pas de dégager des regroupements nettement délimités dans l'espace.

Mots-clés : inversion thermique, topographie, distance à la mer, régression, classification ascendante hiérarchique (CAH), interpolation.

Abstract – Our database comprises daily minimum and maximum temperatures observed over 10 years at 859 pairs of meteorological stations throughout France. Each pairing associates a low and a high station. The influence of six predictors on the intensity, frequency, and duration of temperature inversions is measured by linear regressions. Five predictors are drawn from a 250 m-resolution DTM: elevation, depth of the valley where the low stations are located, magnitude of positive relief (ridge, hills), gradient of the slope of the hill or mountainside, and altitudinal amplitude between the high and the low station. The sixth descriptor used is the distance to the nearest sea. Topography exerts a major influence over the formation of thermal inversions. Three of the descriptors account for more than 80% of the variance of the inversion characters: distance to the sea, valley depth, and altitudinal amplitude. Elevation explains only 24% of that variance. The spatial distribution of the three characteristics of the inversions highlights several categorizations that fit into several nested scales. The 859 sites can be arranged into three classes relating to mountains, coastal areas, and plateaus. However, their distribution over the area under consideration is unclear and fails to indicate sharply delimited groupings.

Keywords: thermal inversion, topography, distance to the sea, regression, Ascending Hierarchical Classification (AHC), inversion mapping.

* Auteur de correspondance : daniel.joly@univ-fcomte.fr

Introduction

Thermal inversion phenomena frequently develop in the first few metres above the ground surface (Barry, 2008). Inversions are classified by the mechanisms that generate them: subsidence inversions, advective inversions, contact inversions, and radiative inversions (Busch *et al.*, 1982). Whatever their type, inversion phenomena are initiated or reinforced by local topography (Anquetin *et al.*, 1998; Fallot, 2012). Because it is denser than warmer air, cold air migrates down

slopes and accumulates at the bottom of depressions (Helmis and Papadopoulos, 1996; Papadopoulos and Helmis, 1999; Mahrt *et al*., 2010; Fernando *et al*., 2013; Burns and Chemel, 2015). The boundary layer that develops in such contexts is totally decoupled from the overlying synoptic flow (Lundquist *et al*., 2008; Daly *et al*., 2010; Dorninger *et al*., 2011; Largeron and Staquet, 2016a). Indeed, within the boundary layer, the surface states partly modulate the thermal fields. However, these fluctuations are difficult to model because they develop at a fine scale where, without a realistic surface representation, Global Circulation Model (GCM) biases are strong (Garratt, 1996). Furthermore, the total impacts of the biases on projected trends depend heavily on regions and cannot be linearly removed (Liang and Qin, 2008).

It is therefore a major challenge to identify meteorological fields within the boundary layer. Moreover, it is within this boundary layer that pollution is the worst and that most plant and animal life is to be found. This is why these mechanisms generate a great deal of attention, for example in France with the Critical Zone Observatories-Application and Research initiative (Gaillardet *et al*., 2018). Regional Climate Models (RCMs), in part thanks to their greater number of vertical levels, make it possible to reduce biases within the boundary layer (Giorgi *et al*., 1993). Nevertheless, despite considerable progress in recent years, output from both Global and Regional Circulation Models is still afflicted with biases to a degree that precludes their direct use, especially in climate change impact studies (Ehret *et al*., 2012; Enayati *et al*., 2021; Tong *et al*., 2021). There are several techniques for correcting bias, but they are all very much open to question. One such technique, geomatic downscaling (Joly *et al*., 2011), can disaggregate GCMs and RCMs to finer resolutions than can be done with dynamic downscaling, although not over small areas, because of the computing time required. Were this to become feasible, we would have far better knowledge of the thermal conditions near the ground surface.

This article seeks to understand the ways in which inversions vary across space in order to identify what is required to predict them. It follows on from a companion paper describing the temporal variations of inversions in France (Joly and Richard, 2022) that confirmed the idea that inversions are not randomly distributed over space. Some regions – the Alps under certain conditions, the coastlines under other conditions – experience inversions of higher intensities, frequencies, and durations than others. It is this aspect of the proclivity of certain places to inversions that is considered here.

The objective of the article is to identify the places in mainland France (excluding Corsica) where inversions are the most intense, most frequent, and longest lasting. Special attention will be given to the influence of topography on these three characters by (*i*) identifying the topographic factors that explain the spatial variation of inversions and (*ii*) evaluating their influence. The data are made up of daily minimum and maximum temperatures and a high-resolution digital terrain model (DTM) is used to construct variables to describe the shape of relief. Multiple regressions are mobilized to spatially interpolate the point data and to develop fine-scale maps of the intensities, frequencies, and durations of inversions throughout France. Ascending Hierarchical Classification (AHC) is then used to analyze the spatial structures of inversion characteristics. The discussion section criticizes and interprets the findings.

1. Data

The study area and the data are presented in detail in Joly and Richard (2022), section 1.1. 'Data', 1.2. 'Method', and 2.2. 'Pairing characters'). They are briefly recalled here. We selected the 1097 Météo-France stations available in mainland France over the period 2008–2017 (3653 daily minimum – tn – and maximum – tx – temperatures). This span of time is long enough to avoid overdependence on the interannual variability of weather conditions, while maintaining as many stations as possible, given that many stations have been opened or, on the contrary, closed in recent decades.

The calculation of inversions is based on the temperature difference between two stations forming a pair. The first criterion for pairing two stations is the Euclidean distance between them that must not exceed 30 km; the reasons for this choice of distance are given in Joly and Richard (2022) in sections 1.2.1. and 2.1. The second criterion is the

altitude difference between the two stations that must be at least 100 m. So, each pair consists of a low station and a high station. A final filter was applied and only those stations with a shortfall of less than 10% of temperature readings (tn and tx) were selected. In the end, a total of 859 pairs were used (figure 1).

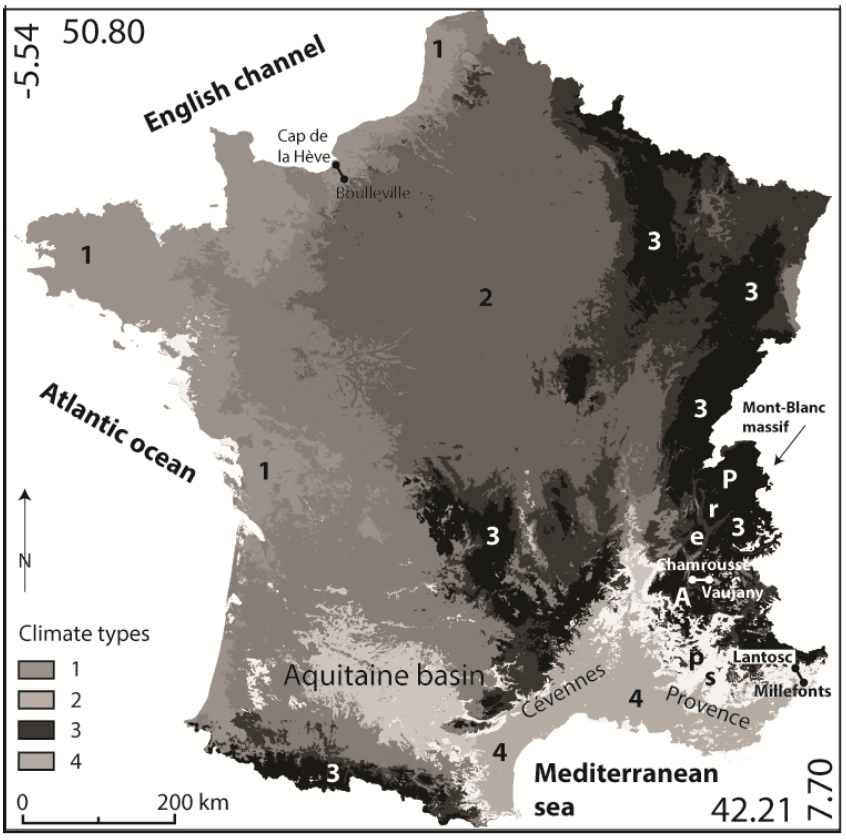

Figure 1. Study area; places named are those discussed in the paper. Type 1 = largely pure oceanic; type 2 = degraded oceanic; type 3 = mountain; type 4 = Mediterranean. *Zone d'étude ; les lieux nommés sont ceux discutés dans l'article. Type 1 = océanique largement pur ; type 2 = océanique dégradé ; type 3 = montagne ; type 4 = méditerranéen.*

Processing required data from France's Institut Géographique National (IGN). The database uses spatial references in raster mode covering the country at a resolution of 250 m and is managed by a Geographical Information System (GIS). Several descriptors were derived from the Digital Terrain Model (DTM). In accordance with the results of Joly *et al*. (2012), Joly *et al*. (2018), and Joly and Richard (2018), five topographic descriptors were first chosen: elevation of the low station [*elev*], depth of the valley where the low stations are located [*valley*], magnitude of positive relief (ridge, hills) where the high stations are located [*hump*], gradient of the slope of the hillsides or mountainsides where the low stations are located [*slope*], altitudinal amplitude between the high station and the low station [*amplit*]. A sixth descriptor is used, the distance to the nearest sea [*dist sea*]. Finally, the typology of climates in France derived from the work of Joly *et al*. (2010) was used. Four types were selected: largely pure oceanic, degraded oceanic, mountain, and Mediterranean. All data layers were projected in the Lambert 93 system.

2. Method

The methodological aspects are mainly based on single and multiple regressions. The variables explained are the indicators of the inversions: intensity, frequency, and duration for tn and tx. The terminology relating to the durations of the inversions is defined in Joly and Richard (2022). In summary, the first way to consider duration is to identify isolated inversions which occur occasionally and are of two types. An isolated tn inversion is

neither preceded nor followed by a tx inversion. An isolated tx inversion is neither preceded nor followed by a tn inversion. If such inversions recur on the following day or over several successive days, they form what are called 'isolated inversion sequences', which will later be referred to as simply 'tn-sequences' or 'tx-sequences' according to the time of day when they occur. The second way is to identify inversions extending over more than half a day: a tn-inversion preceded or followed by a tx-inversion, or a tx-inversion preceded or followed by a tn-inversion are referred to as 'persistent inversions'.

The explanatory variables are the topographic descriptors (*elev*, *valley*, *hump*, *slope*, *amplit*, and *dist sea*) expressed in linear, polynomial, or logarithmic forms. These three forms of regression adjustment are systematically tested, the one that returns the highest determination coefficient (R^2) being selected. The inversion characteristics are estimated from two types of regression:

- The global regression covers the whole corpus of 859 sites.
- Local regression is based on the segmentation of space into a large number of small spatial units (Joly *et al*., 2011). This method is implemented in three main steps: (1) identification of the 30 stations closest to the point of estimation and division of the territory into polygons according to a neighborhood rule. In our case, France is segmented into 5984 polygons; (2) identification of the significant explanatory variables and analysis by multiple regression within each polygon; (3) application of the coefficients to the pixels making up each polygon (interpolation).

The regression coefficients (Bravais-Pearson R) and the Root Mean Square Error (RMSE) of the residuals from the regressions are used to assess the quality of the estimates. Other values are provided: deviations from the mean over the four seasons and across the four climate types. Maps are drawn for spatially situating the results in France.

3. Results

3.1. Factors explaining the intensity, frequency, and duration of inversions

Tables 1 and 1bis summarize the relations obtained (R values in linear, polynomial, or log forms) among four indicators of inversions (intensity, frequency, length of the isolated inversion sequences, and duration of persistent inversions) and the six predictors (*elev*, *valley*, *hump*, *slope*, *amplit*, *dist sea*). Most correlations are significant at the 5% threshold. Note also that the sign of the correlation can be reversed depending on whether we consider night (tn) or daytime (tx) inversions.

Table 1. Correlation coefficients (R) of the six topographic explanatory variables of the intensity [Intens], frequency [freq], and duration of the inversions [Seq = duration of the inversion sequences, Persist = duration of persistent inversions]; tn, tx = inversions at minimum and maximum temperatures. Significant coefficients at the 10% (*), 5% (**), or 1% (***) threshold. Elev = elevation, valley = depth of valley, hump = magnitude of positive relief, slope = gradient of the slope of the hillsides or mountainsides, amplit = amplitude (difference in elevation between the high and low stations), dist sea = distance to the nearest sea. *Coefficients de corrélation (R) des six variables topographiques explicatives de l'intensité [Intens], de la fréquence [freq] et de la durée des inversions [Seq = durée des séquences d'inversion, Persist = durée des inversions persistantes] ; tn, tx = inversions aux températures minimale et maximale. Coefficients significatifs au seuil de 10% (*), 5% (**), ou 1% (***). Elev = élévation, valley = profondeur des vallées, hump = importance du relief positif, slope = gradient de la pente des versants, amplit = amplitude (différence d'élévation entre les stations haute et basse), dist = distance à la mer ou à l'océan le plus proche.*

	Intens. tn	Intens. tx	Freq. tn	Freq. tx	Seq. tn	Seq. tx	Persist.
R elev	0.69*	0.88***	-0.35	0.1	0.18	0.64*	0.55
R valley	0.97***	0.97***	0.98***	0.86***	0.90***	-0.90***	0.95***
R hump	-0.92***	0.52	-0.98***	0.89***	-0.99***	0.88***	-0.98
R slope	-0.84**	0.73**	-0.89***	0.65*	-0.44	0.68*	0.50
R amplit	0.98***	0.95***	0.98***	0.66*	0.96***	-0.82***	0.93***
R dist	0.89***	-0.93**	0.99***	-0.95***	0.97**	-0.95***	0.99***

Table 1bis. Shape of fit linear [lin], logarithmic [log], or polynomial of order 2 [Polyn 2] of the six topographic explanatory variables. The meaning of the abbreviations is given in Table 1. *Forme de l'ajustement linéaire [lin], logarithmique [log], ou polynomial d'ordre 2 [Polyn 2] des six variables explicatives topographiques. La signification des abréviations est donnée dans le tableau 1.*

	Intens. tn	Intens. tx	Freq. tn	Freq. tx	Seq. tn	Seq. tx	Persist.
Elev	Polyn 2	Polyn 2	lin	lin	lin	Polyn 2	lin
Valley	log	lin	log	Polyn 2	log	log	lin
Hump	log	lin	log	lin	log	lin	log
Slope	lin	lin	lin	lin	lin	lin	lin
Amplit	log	lin	lin	polyn 2	log	log	lin
Dist	Log 50 km	Log 25 km	Log 12.5 km	Log 50 km	Lin 12.5 km	Lin 12.5 km	Lin 25 km

3.1.1. Elevation

Elevation is associated with the intensity of the inversions (tn and even more so tx), and secondarily the duration of the tx-sequences (table 1). The polynomial form reveals a complex relationship between the variables when compared two by two. This point will be developed in the discussion section. On the other hand, the frequency of inversions is not correlated with elevation. Globally, this descriptor explains only a small proportion of the inversions ($r < 0.18$).

3.1.2. Valley depth

The depth of the valleys at the bottom of which the low stations are located is highly explanatory for all five inversion indicators (table 1). In some cases (intensity tn, frequency tn), the fit is almost perfect. The log form almost always fits the distribution better than the linear form. Note that the relationship between valley depth and frequency of tx-inversions follows a polynomial pattern reflecting a complex relationship. Deep valleys make for more intense and more frequent nocturnal and diurnal ($R>0$) inversions. On the other hand, valley depth is associated with long tn-sequences and short tx-sequences. Night and daytime inversions are thus separate events. Finally, deep valleys allow the formation of long-lived inversions.

3.1.3. Hump magnitude

The magnitude of the relief on which the high stations are located also has a determining role on all indicators of inversions (table 1). The magnitude of the relief explains in particular more than 95% of the spatial variation of the frequency of tn-inversion sequences, tx-sequences, and persistent inversions. Only the intensity of tx-inversions is little affected by the magnitude of positive relief. It should be noted that the role of the magnitude of relief is systematically reversed between night and daytime inversions, *i.e.* the sign of the coefficients changes between tn and tx on the correlations obtained with the four indicators (intensity, frequency, length of sequences, and duration of persistent inversions). The more the reliefs emerge, the lower the value of the characters for the tn-inversion and the reverse is observed for the tx-inversion. Note that the most suitable form of fit is logarithmic for the tn-inversion. The logarithmic form indicates that the decrease in the values of tn-inversions (intensity, frequency, and duration) and persistent inversions is not regular. Values of inversion are higher for small hump amplitudes than for large ones. This differentiated influence is not found with the values of tx-inversions whose progression follows linearly that of positive reliefs, whatever their size.

3.1.4. Slope of the hillsides or mountainsides

For this predictor again, the reversal in the sign of the correlation is systematic between nocturnal and diurnal inversions. Steep slopes are not conducive to tn-sequences but are favorable to tx-sequences and persistent inversions. The gradient of the slopes on which the low stations are installed mainly influences the indicators of tn-inversions. When the low stations are located on a slope, the inversions are weaker, less frequent and shorter-lived than when they are located at the bottom of a trough. Cold air does not accumulate there. The fact that the steep slopes are located in the mountains reinforces this relationship. The positive correlation between slope and tx-inversions, while weaker than

for tn-inversions, is more difficult to interpret. The linear shape of the slope inclination values is the one that best fits the characters of the inversions.

3.1.5. Elevation amplitude

The difference in elevation between the two stations making up each pair is also a determining factor. All correlation coefficients are positive, except for the duration of the tx-sequences (R=-0.82). A high amplitude reflects the magnitude of the relief present only in the mountains, the site of the most intense, frequent, and long-lasting inversions. The exception, the duration of the tx-sequences, seems to occur outside mountain areas.

3.1.6. Distance to the nearest sea

The distance to the nearest sea has an almost absolute influence on all indicators, but within a more or less wide buffer zone between the coast and a distance of 5 km (duration of inversions) to 50 km (frequency of tn-inversions, intensity of tx-inversions). The logarithmic form of the distance is the one that best fits the frequencies and intensities of the inversions: the influence of the sea, which is very strong towards the coast, fades away increasingly rapidly with distance from it. The duration of the inversions is best fitted by the linear form. The influence of the distance to the sea is systematically reversed between night and daytime inversions. The nocturnal inversions are thus continental whereas the diurnal ones are maritime. Persistent inversions are nocturnal and continental.

3.2. Characters of inversion modeling

Multiple regressions make it possible to model (estimate and map) the characters of the inversions (intensity, frequency, and duration) in relation to the shapes of the relief. The characters of the inversions are the variables to be explained and mapped at any point of the space considered (France). They are known for 859 sites each made up of a pair of stations. The characteristics at the low point (altitude, magnitude of the positive relief and depth of the valleys where the low point is located, slope, distance to the sea) are taken into account as explanatory variables.

3.2.1. Inversion character estimates by multiple regressions

Global multiple regressions provide low R^2 and high RMSE values (table 2). Only the intensity of the tn and tx-inversions exhibits R^2 values greater than 0.1 (0.14 and 0.27 respectively). This poor performance is due to the climatic and topographic diversity of the studied area which is composed of pure or degraded oceanic and Mediterranean climates, mountains with contrasting topography, plains and plateaus with rounded relief, and coastal fringes (Joly *et al*., 2010). The statistics produce a general model disturbed by inevitable contradictory effects in such varied contexts. To overcome this difficulty, we use local interpolation which, by searching for information within a geographically restricted space, adjusts the regression parameters much more reliably than with global regressions.

The resulting interpolation performance is higher as no R^2 is less than 0.24 and the maximum R^2 (tx-inversion intensity) is equal to 0.7 (table 2). For example, the R^2 values of the inversion frequencies (tn and tx) change from global to local regressions from 0.06 and 0.01 to 0.43 and 0.37. Local regressions reduce the adjustment errors. The RMSE of the inversion frequencies (tn and tx) change from global to local regressions from 17.3 and 14.4 to 13.5 and 11.4.

Table 2. R^2 and RMSE of the seven characters of inversions (glob = global, loc = local). Intens = intensity of inversions, freq = frequency of inversions, Seq = duration of inversion sequences, Persist = duration of persistent inversions; tn, tx = inversions at minimum and maximum temperatures. *R^2 et RMSE des sept caractères des inversions (glob = global, loc = local). Intens = intensité des inversions], freq = fréquence des inversions, Seq = durée des séquences d'inversion, Persist = durée des inversions persistantes ; tn, tx = inversions aux températures minimale et maximale.*

	Intens. tn	Intens. tx	Freq. tn	Freq. tx	Seq. tn	Seq. tx	Persist.
R^2 glob	0.14	0.27	0.06	0.01	0.07	0.01	0.1
R^2 loc	0.45	0.70	0.43	0.37	0.43	0.24	0.32
RMSE glob	10.8	6.6	17.3	14.4	10.8	2.6	4.6
RMSE loc	8.5	1.1	13.5	11.4	0.58	0.11	0.19

While comparable improvements in intensities are observed, local regressions are of the greatest interest in the sequences: the RMSE increases from 0.58 (local regression) to 10.8 (global regression) days when estimating the duration of tn-sequences.

3.2.2. Characters of inversion mapping

The highest tn-inversion intensities are found at the bottom of the valleys located in the southern two-thirds of France. These valley bottoms may be situated in plains (Aquitaine Basin), around mountainous massifs (Vosges, Prealps), or in the heart of mountain ranges (Alps) (figure 2A). The coastal fringe from northern France to Vendée (including Normandy and Brittany) has low tn-inversion intensities. These low intensities are also found in the heart of all mountain ranges: Vosges, Massif Central, Alps, and Pyrenees (figure 1 for locations).

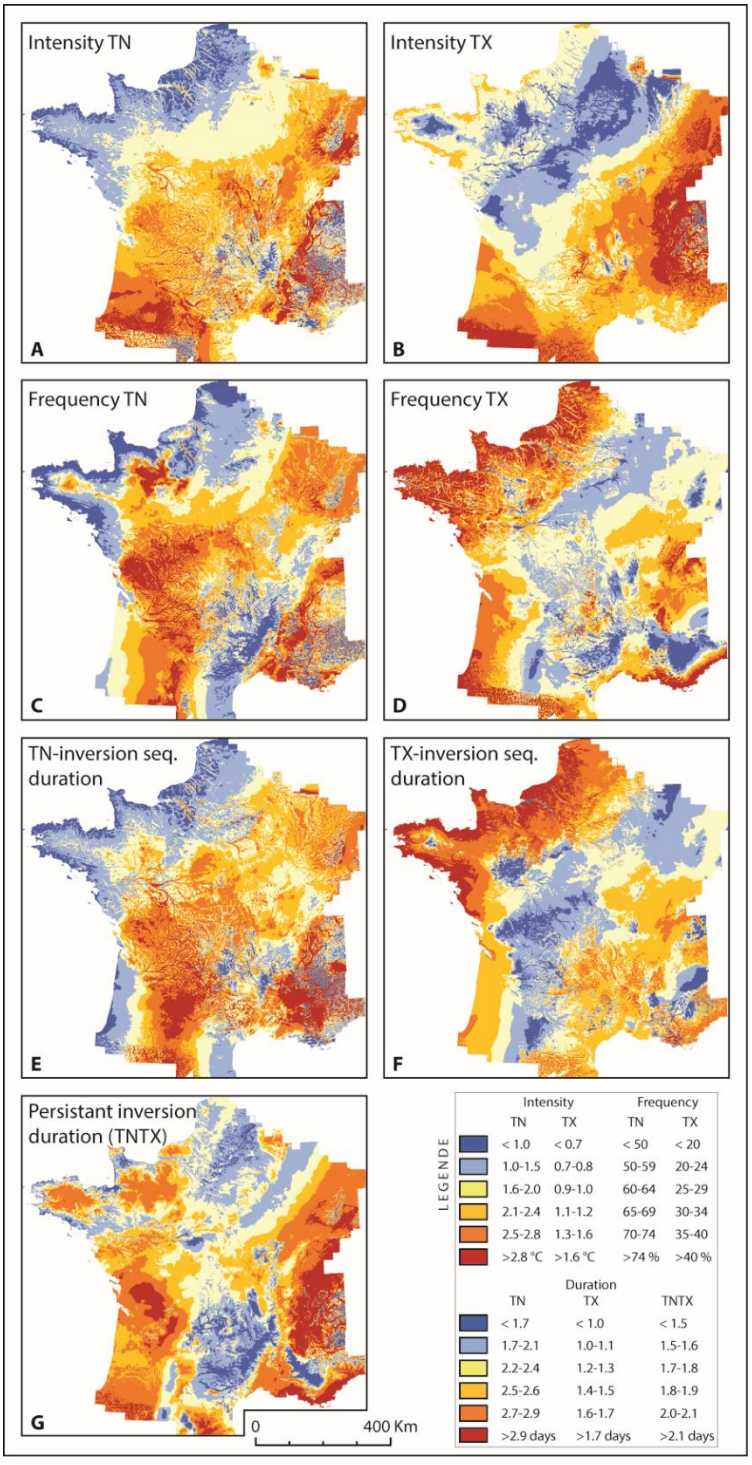

Figure 2. Estimation of the intensity and frequency of inversions that occur at tn and tx; duration of inversion sequences that occur at tn and tx; duration of persistent inversions. *Estimation de l'intensité et de la fréquence des inversions qui se produisent lors des tn et des tx ; durée des séquences d'inversion qui se produisent lors des tn et des tx ; durée des inversions persistantes.*

The intensities of the tx-inversions (figure 2B) have homogeneous ranges that are wider than those of the tn-inversions (figure 2A). The highest intensities are found in eastern France (Vosges, Jura, Rhône Valley, Prealps and Alpine valleys) and in the Pyrenees (figure 2B). The whole Paris Basin and its extension towards the Loire Valley and Vendée, as well as the centre of Brittany, have low tx-inversion intensities.

The spatial distribution of high tn-inversion frequencies concerns several regions that are far apart and differ in terms of their topographic or climatic characteristics: Mont-Blanc Massif, Prealps, the centre west, and part of Normandy to the north (figure 2C). The entire coastal fringe of the English Channel and Brittany as well as the Cévennes have low tn-inversion frequencies. Almost everywhere, valley bottoms with high values are opposed to ridges and upper slopes where inversions are rare: this is why the southern Alps juxtapose a multitude of small, elongated, contrasting sectors with alternately high and low frequencies. The high tx-inversion frequencies (figure 2D) are preferentially located beside the seas (north, west, and the Mediterranean basin) while the interior of the country exhibits lower values except for a few mountain areas (Jura, Northern Alps, Massif Central, Pyrenees).

The spatial distributions of the tn- (figure 2E) or tx-sequences (figure 2F) are the inverse of each other: short (tn) or long (tx) inversion periods along the English Channel and Atlantic Ocean, and much longer (tn) or shorter (tx) sequences in the interior. The longest durations of persistent inversions are characteristic of the Mediterranean periphery, the mountain ranges (except for the highest peaks), and the Charente (figure 2G). The shortest durations are found in the Massif Central, inland Provence, and northern France, with the exception of inland Brittany and Normandy.

3.3. Typology of sites with regard to inversions

The set of maps highlights large geographical regions (mountain ranges, coastal areas, etc.), but none of these areas appears to be homogeneous. For tn as for tx, intensities, frequencies, and durations of inversions can vary very greatly over short distances, within each of the large geographical regions. An Ascending Hierarchical Classification (AHC) ranks each of the 859 sites according to the characters of the inversions. Based on the dendrogram (not shown), three classes are recommended. Classes 1, 2, and 3 respectively group 47%, 22%, and 31% of the sites. The average of the six topographic characters is calculated for the 859 sites in the three classes (table 3). This calculation makes it possible to characterize the average topographic context of all the sites and each of the classes. From this AHC, the calculation of a dimensionless metric (interclass amplitude divided by the average) can be used to rank the six topographic characters. Three of them are strongly discriminated by the AHC (valley, hump, and amplit).

Based on a similar principle, Table 4 presents the mean values of the inversion characters. This calculation makes it possible to characterize the inversion profile of each of the classes.

Table 3. Average values of the six topographic characters for the three classes and the mean; and dimensionless metric (*: interclass amplitude divided by the average) in each class. Bold = above average; underlined = below average; neither = near average. *Valeurs moyennes des six caractères topographiques données pour les trois classes et la moyenne ; et métrique sans dimension (* : amplitude interclasse divisée par la moyenne) dans chaque classe. Gras = supérieur à la moyenne ; souligné = inférieur à la moyenne ; ni l'un ni l'autre = proche de la moyenne.*

	Elev (m)	Valley (m)	Hump (m)	Slope (°)	Amplit (m)	Dist sea (km)
Cl1	471.1	**187.1**	12.0	5.9	**635.5**	**190.9**
Cl2	**478.5**	70.4	**44.0**	**7.7**	275.8	137.3
Cl3	455.1	68.9	27.3	5.6	327.3	173.2
Mean	467.7	124.8	23.8	6.2	461.0	173.7
Amp/mean	0.05*	0.95*	1.34*	0.34*	0.78*	0.31*

Table 4. Average values of the inversion characters in each class. Bold = above average; underlined = below average; neither = near average. *Valeurs moyennes des caractères d'inversion dans chaque classe. Gras = supérieur à la moyenne ; souligné = inférieur à la moyenne ; ni l'un ni l'autre = proche de la moyenne.*

	Intens. TN (°C)	Intens. TX (°C)	Freq. TN (%)	Freq. TX (%)	Seq. TN (Day)	Seq. TN (Day)	Persist. (Day)
Cl1	2.9	**2.0**	**78.0**	**33.8**	**3.3**	1.1	**2.1**
Cl2	**3.6**	1.2	40.2	11.6	1.5	**1.5**	1.6
Cl3	2.0	1.8	65.5	21.7	2.7	1.1	1.5
mean	2.8	1.5	65.9	25.2	2.7	1.2	1.8

Class 1 includes sites with a topographic context combining low humps and deep valleys at low stations, high amplitudes between high and low stations, and remoteness from the sea (table 3). Note that the slope gradients are slightly lower than average, lending credence to the hypothesis of low stations being located preferentially in flat areas, including valley bottoms. For this class 1, inversions are intense, tn and even more so tx, and frequent, especially for tn (table 4). The tn-sequences are long and lasting. The sites concerned by this class are preferentially located in the southeast diagonal of France, inland in mountain valley bottoms (figure 3A). This class is typically mountainous, Alpine and Pyrenean, but also characteristic of the lower mountain ranges (Massif Central and Vosges)

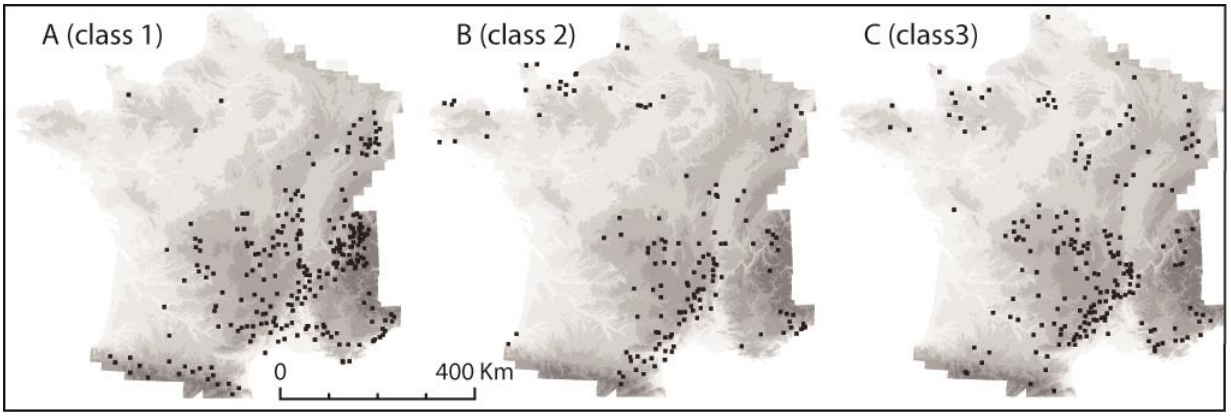

Figure 3. Location of stations belonging to each of the three classes resulting from an ascending hierarchical classification based on the topographic characteristics of the 859 sites. *Localisation des stations appartenant à chacune des trois classes résultant d'une classification hiérarchique ascendante portant sur les caractères topographiques des 859 sites.*

Class 2 includes sites generally characterized by inverse indicators. It combines the following opposing characters (table 3): high amplitude of humps, and shallow valleys at the low station, and low amplitudes between high and low stations. Steeper than average slope gradients (7.7°) suggest that the low stations are mostly located on slopes rather than in valley bottoms. The difference between the two sensors is small as is the average depth of the valley where the low station is located. The characteristics of the inversions show lower than average values except for the intensity of the tn-inversions and the duration of the tx-sequences (table 4). Several low stations of this class are located on the coastline, particularly close to the English Channel (figure 3B). This type of site is undoubtedly marked by sea breezes which would limit the diurnal warming of the low stations. But this type goes beyond the coastal framework and includes regions where cloud cover may persist during the day: maritime influences over the Languedoc plain or the English Channel coast. It should be noted that several medium mountain regions are also included in this class, particularly the Massif Central.

Class 3 has near-average topographic features (table 3). Only valleys and slopes are slight. This class seems to be typical of plateaus or shallow valleys. Inversion characters are weak to moderate (table 4). This class occurs throughout France with a fairly high density along the eastern edge of the Massif Central (Cévennes), in the interior of Normandy and east of the Paris Basin. It is also very much present in Paris, where air pollution could explain the low daytime warming of the low stations located in the heart of the Paris conurbation (figure 3).

4. Discussion

4.1. Factors explaining the characters of inversions

The maps of the estimates of the three indicators of inversions reveal two main distribution patterns across France (figure 2). The tn-inversions exhibit low intensity, frequency, and duration values along a coastal fringe of the English Channel and the Atlantic Ocean, whose width, about 200 km to the north, narrows towards the west and south. The southern part of the Massif Central also displays weak values that vary in extent for the different indicators. The highest values extend from the NE to the SW across the north of the Massif Central. They also affect all the Prealps. The Alps themselves are characterized by a mosaic of sectors with contrasting values. The tx-inversions are the reverse of the previous ones: high values along the coasts and low values inland.

This distribution results from the response of inversion indicators to the stimuli exerted by topographic factors (figure 4). Values of the inversions (intensity, frequency, duration) occurring in the mornings fall as the hump and slope gradient values rise: low stations located on salient ridges or peaks or on steep slopes present tn-inversions that are weak, infrequent, and short-lived sequences. The opposite is true for tx-inversions, which are more frequent when the stations are located on exposed relief.

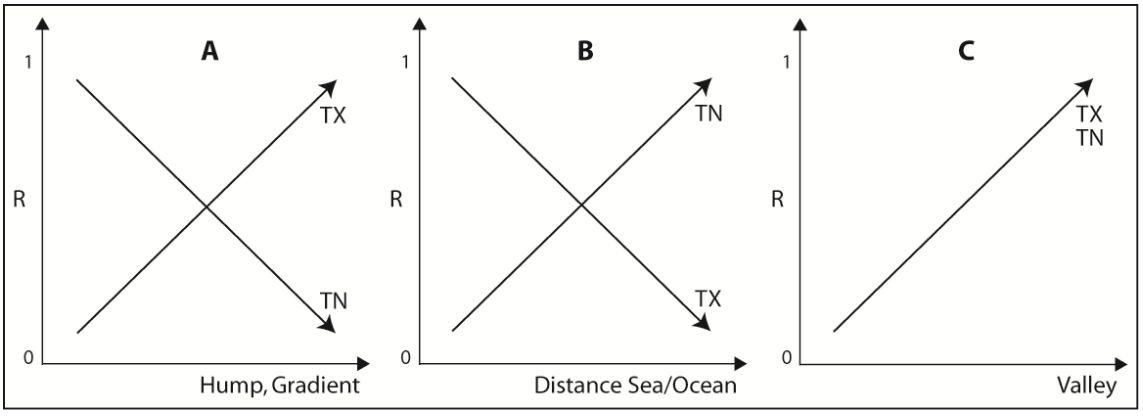

Figure 4. Variation of the correlation coefficient (R) between the value of the three inversion indicators (intensity, frequency, duration) and (A) the emergence of landforms and slope, (B) the distance to the nearest sea, and (C) the depth of valleys. *Variation du coefficient de corrélation (R) entre la valeur des trois indicateurs d'inversion (intensité, fréquence, durée) et (A) l'émergence des reliefs et pente, (B) la distance à l'océan ou la mer le plus proche et (C) la profondeur des vallées.*

The distance to the nearest sea works in the reverse direction. The values of the tn-inversions are weak near the sea and higher with distance from the coast; those of tx-inversions are high near the sea and decrease as a direct function of distance from the coast. The logarithmic relationship between distance to the sea and the intensity and frequency of inversions exhibits opposing signs for tn and tx-inversions. This raises the hypothesis of a link with coastal breeze cells (Planchon and Cautenet, 1997).

The depth of the valleys is a powerful factor dictating the intensity and frequency of both tn and tx-inversions. The respective influences of humps and valleys could indicate that valley bottoms, and especially the deep valleys, are more disconnected from synoptic conditions than crests and upper slopes.

The distance between the two stations of each site is another candidate variable that could have been taken into account to analyse the characteristics of inversions. It might have allowed a better evaluation of the influence of distance on the detection of inversions. It is indeed reasonable to think that the heterogeneity of climatic conditions (sunshine, temperature, etc.) increases with distance and thus that two stations 25–30 km apart are more different than two stations less than 10 km apart. We did not take this variable into account in our analyses because, unlike landforms, it cannot be used in modelling (estimating and mapping) the characteristics of inversions.

4.2. Forms of inversion character adjustment

The characteristics of the inversions (intensity, frequency, and duration) were estimated by six predictors (section 3.2.). Among the three forms of fit selected, linear fit is the most frequent (50%) followed by logarithmic fit (40%). The second-order polynomial fit is retained four times (10%). As an illustration, we have chosen the valley predictor which adjusts the characters of the inversions according to the three types of fit (figure 5).

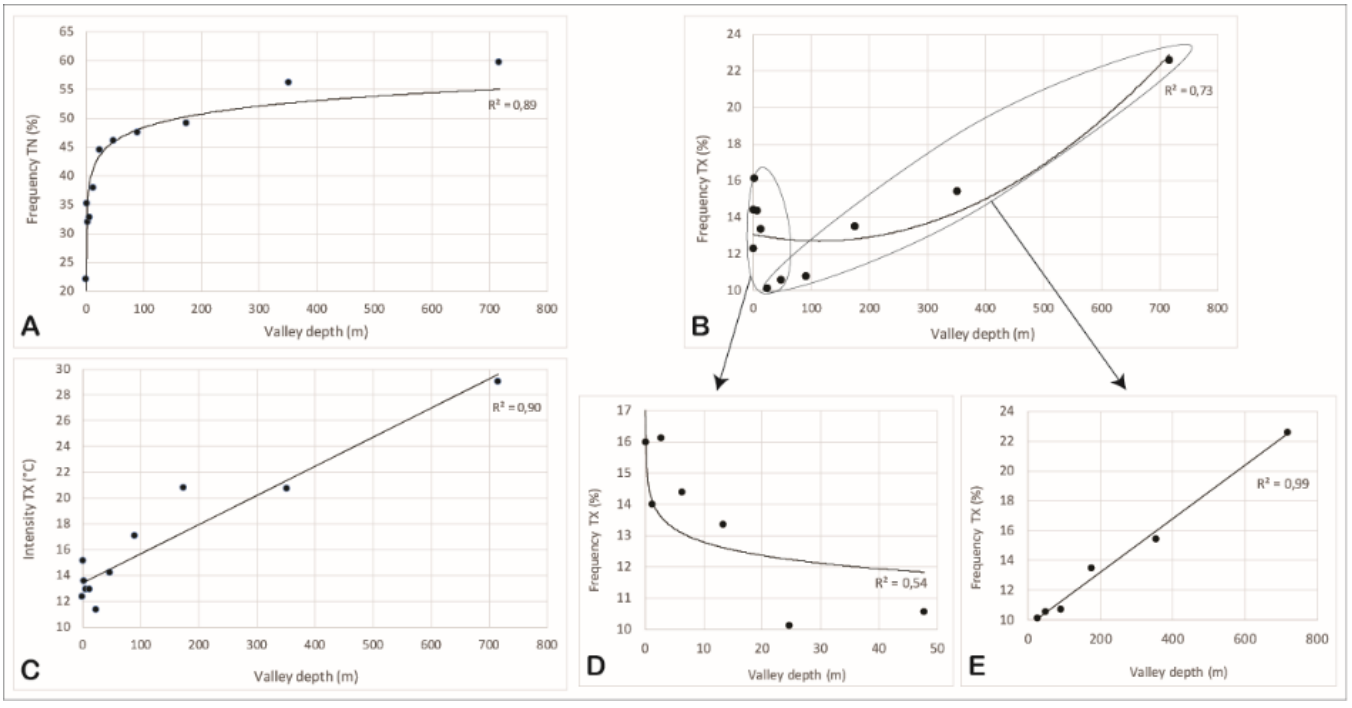

Figure 5. The three forms of inversion characteristic adjustment by valley depth. The valley depths are segmented into 11 classes in a geometric progression; the average of each class is plotted on the x-axis. The average depth of valleys for each class is plotted on the y-axis. The frequencies of the tn-inversions are fitted in logarithmic form (A); those of the tx-frequencies and tx-intensity in second-order polynomial form (B), and linear form (C). The polynomial form is decomposed into its two segments: decreasing for low depth values (D) and increasing for high depth values (E). *Les trois formes d'ajustement des caractéristiques d'inversion pour la profondeur des vallées. Les profondeurs des vallées sont segmentées en 11 classes selon une progression géométrique ; abscisses = profondeur moyenne des vallées pour chaque classe ; ordonnées = moyenne des caractéristiques d'inversion pour chaque classe. Les fréquences des inversions tn sont ajustées sous forme logarithmique (A) ; celles des fréquences tx et de l'intensité tx sous forme polynomiale du second ordre (B) et sous forme linéaire (C). La forme polynomiale est décomposée en ses deux segments : décroissante pour les faibles valeurs de profondeur (D) et croissante pour les fortes valeurs de profondeur (E).*

The logarithmic form suggests a differentiated increase in the frequency of tn-inversions (figure 5A). For deeper valleys, the frequency varies little. This form of adjustment also characterizes the magnitude of the positive relief and the distance to the sea (table 1).

The polynomial shape fits a variation in the frequency of the tx-inversion which seems to be split into two parts (figure 5B). Up to a depth of 100 m, the frequency decreases in a logarithmic form (figure 5D); beyond a depth of 100 m and up to depths greater than 600 m the frequency

increases linearly (figure 5E). Elevation adjusts the characters of the inversions most often (three times) according to the polynomial form (table 1).

The linear form is simple (figure 5C). The intensity of the inversions increases in proportion to the depth of the valleys. This linear form is most often the best fit for the character of the inversions in terms of the elevation and gradient of the slopes (table 1).

4.3. Mean deviation of the three inversion indicators according to four types of climate

The companion paper (Joly and Richard, 2022) establishes the average monthly variations in the intensity, frequency, and duration of the inversions. The graphs presented result in the form of averages calculated for the 859 sites. The problem then arose as to whether the monthly rhythms of these indicators were uniform or whether they differed across climates. To answer this question, we classified the 859 study sites by the climate to which they belong among the eight inventoried in France (Joly *et al*., 2010) and then reproduced the previous calculations within the framework of each of them. The results of the calculations are presented below in the form of deviations from the mean, the latter corresponding to the values established by Joly and Richard (2022).

The intensity of the tn-inversions is consistent with the French average (low deviation from the average) for mountain, degraded oceanic, and Mediterranean climates (figure 6A). The oceanic climate is characterized by nocturnal inversions of much lower intensity. The intensity of the tx-inversions varies little from one season to the other and with small deviations from the average for degraded oceanic and Mediterranean climates, but varies greatly and in opposite directions for mountain and pure oceanic climates (figure 6C).

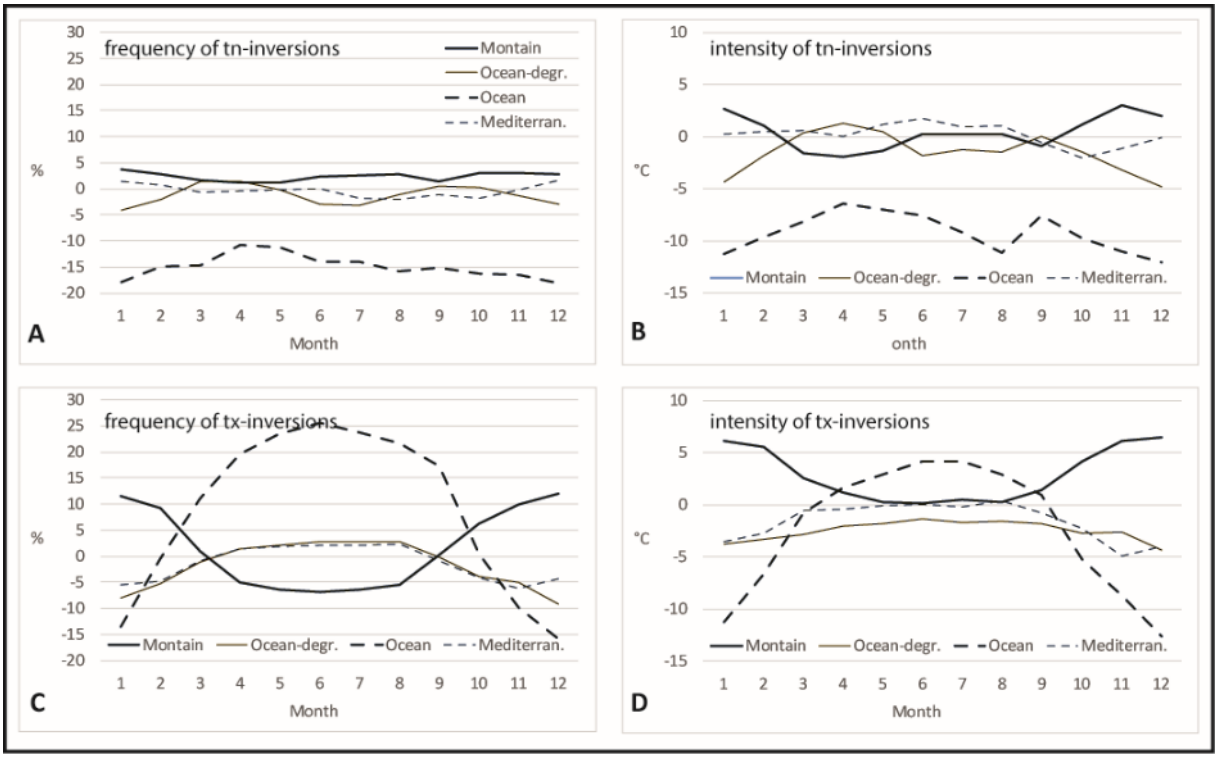

Figure 6. Deviation from the monthly average of the intensity and frequency of the tn and tx-inversions according to four types of climate (mountain, pure oceanic, degraded oceanic, and Mediterranean). *Ecart à la moyenne mensuelle de l'intensité et de la fréquence des inversions tn et tx en fonction de quatre types de climat (montagnard, pur océanique, océanique dégradé et Méditerranéen).*

As with intensity, the frequency of morning inversions (tn-inversions) shows remarkable uniformity in the monthly averages for sites belonging to mountain, degraded oceanic, and Mediterranean climates. Deviations are narrow, in the range -5% to +5% from the mean (figure 6B). Only sites belonging to the pure

oceanic climate show frequencies well below the average, ranging from -17% (winter) to -11% (spring). For the frequencies of tx-inversions, the same contrasting patterns as those observed for intensity appear (figure 6D). The sites belonging to the oceanic climate contrast winter with below-average frequencies (-15%) with the months of April to September during which the differences are very positive (from +20% to +25%). The degraded oceanic and Mediterranean climates show a similar pattern to the pure oceanic climate with very small deviations from the average (-5 to +3%). With the mountain inversions, the oceanic pattern is reversed but with deviations from the mean that are half the size; positive deviations from the mean in winter (+12%) and negative from April to August (-6%).

Figure 7 is based on the same calculations applied to the durations of sequences and persistent inversions. We find the same structures as for intensity and frequency, in particular the oppositions between mountain climate sites and oceanic climate sites, or similar patterns between degraded oceanic and Mediterranean climate sites. For the oceanic climate, durations are minimal in summer for tn-sequences and maximal for tx-sequences and persistent inversions. For mountain climates, the opposite is again observed.

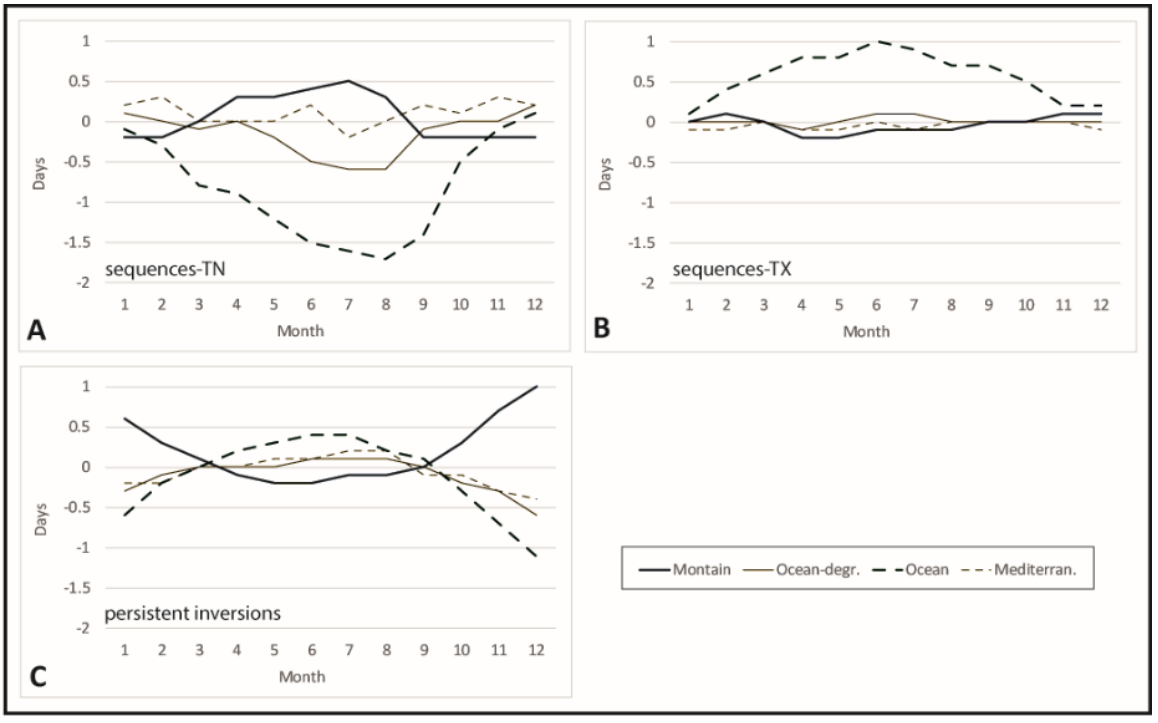

Figure 7. Deviations from the monthly average of inversion sequences and duration for each of the four climates (mountain, pure oceanic, degraded oceanic, and Mediterranean) and the twelve months of the year. *Écarts par rapport à la moyenne des séquences et de la durée des inversions pour chacun des quatre climats (montagnard, pur océanique, océanique dégradé et Méditerranéen) et des 12 mois de l'année.*

In the mountains, the three inversion indicators generally exhibit maximum values in winter, with the sole exception of the tn-sequences. For the oceanic climate, the indicators peak in summer, again with the same exception. In winter, the inversion layer holds up better during the day in mountain valleys, which reinforces the inversions. For the oceanic climate, the intensity and frequency of tx-inversions, as well as the duration of persistent inversions, are stronger in summer, because the waters of the Atlantic Ocean and the English Channel are cooler than the continental air. This impacts coastal stations selected as low stations. In winter, the ocean is warmer than the continent and inversions are weak and rare. The same applies to the Mediterranean climate, in a less marked way. The difference between sites with oceanic and Mediterranean climates can be interpreted in two ways. The relief is more marked on the Mediterranean coasts. The prevailing winds come from the open sea on the Atlantic and the English Channel coasts.

4.4. Physionomy of the longest inversion sequences

The companion paper on inversions (Joly and Richard, 2022) reveals that sequences of successive days with (*i*) a tn-inversion (morning inversion destroyed during the day) or (*ii*) a tx-inversion (afternoon inversion only), and (*iii*) persistent inversions vary greatly in length. Their duration also varies across space: they are preferentially located south of the Alps for the first, north of the Alps for the second, and along the coasts of the English Channel for the third. This is in line with the results found for the classification of sites.

An illustration of the temporal and spatial variations of different types of inversions is proposed in Figure 8.

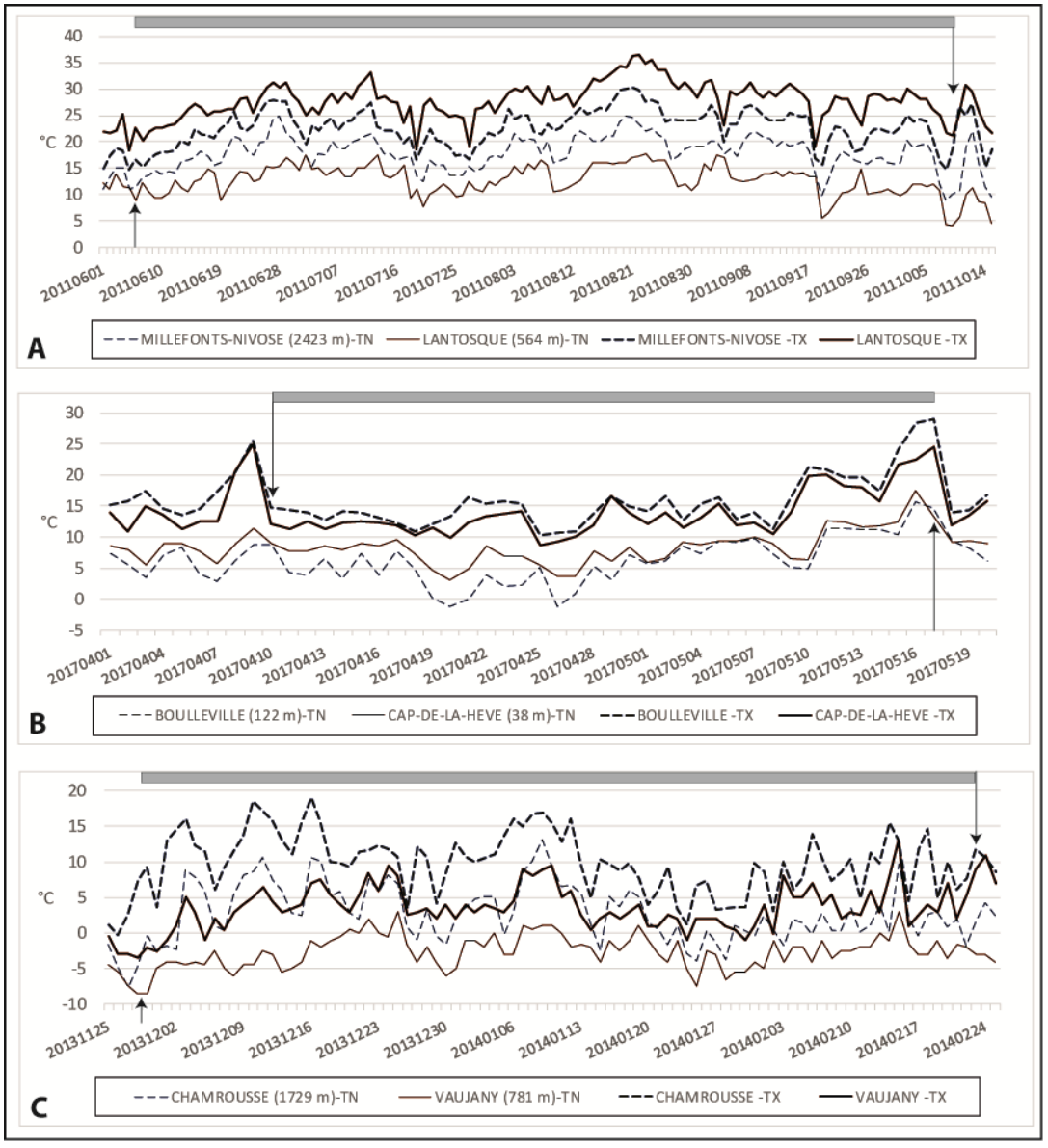

Figure 8. Tn and tx temperatures at the low station and high station of three sites. Dashed line = top station, solid line = bottom station; the arrows mark the beginning and the end of the inversion, the grey bar indicates the period of time during which the inversion lasted: 126 days, from 6 June to 9 October 2011 for the longest tn-sequence (A), 37 days, from 9 April to 17 May 2017 for the longest tx-sequence (B), and 88 days from 28 November 2013 to 23 February 2014 for the longest persistent inversion (C). *Températures tn et tx à la station basse et à la station haute de trois sites. Ligne pointillée = station supérieure, ligne pleine = station inférieure ; les flèches marquent le début et la fin de l'inversion, la barre grisée indique le laps de temps au cours duquel l'inversion a duré : 126 jours, du 6 juin au 9 octobre 2011 pour la séquence-tn la plus longue (A), 37 jours, du 9 avril au 17 mai 2017 pour la séquence-tx la plus longue (B) et 88 jours du 28 novembre 2013 au 23 février 2014 pour l'inversion persistante la plus longue (C).*

The longest tn-sequence lasted 126 days, from 6 June to 9 October 2011 (figure 8A). The sequence starts the day after a tx-inversion. It ends when the high station experienced a lower temperature than the low station. The site where this occurred pairs the Lantosque station, located at 534 m at the bottom of a deep valley and 25 km from the Mediterranean, with the Millefonts-Nivose station, located at 2423 m on the crest of a topographic prominence. During this period, the tn temperature curve of Lantosque is consistently below that of Millefonts-Nivose: the temperature is 5.1°C colder on average in the plain than 2000 m higher in the mountains. During tx, the reverse is observed: the high station is invariably colder than the low station according to the normal altitudinal thermal lapse rate. This pattern of inversion variation is typical of the southern Alps where the absence of cloud cover intensifies radiative losses during the night, resulting in a cooling of the lower layers and cold air accumulating in the valley bottoms. During the day, strong solar radiation warms the air in the lower layers. Thermal instability sets in and anabatic winds carry the warm air upwards, and it cools as it rises.

The longest tx-sequence persists for 37 days, from 9 April to 17 May 2017 (figure 8B). It forms at the mouth of the Seine between the low station at Cap de la Hève (38 m, 100 m from the English Channel coast) and Boulleville, the high station located about 20 km inland, at 122 m altitude. The high station has a continuously higher tx during the sequence than that observed on the coast. The average intensity of the inversion is 1.7°C. During tn, the situation reverses and the high station experiences the cooler temperatures (on average -2.2°C). The inversion forming during the day is destroyed at night. But the process involved is not related to the difference in elevation between the two stations. The inversion that occurs during tx is due to the inertial effect of the sea on the air, whose temperature rises less quickly during the day than inland. Here we find the influence of the distance to the sea, an explanatory variable whose weight has been seen in the spatial variation of the frequency of inversions (section 3.1.; table 1).

The maximum duration of persistent inversions is 88 days from 28 November 2013 to 23 February 2014 (figure 8C). This concerns a deep valley in the Alps, near Grenoble. The difference between the low station, Vaujany (valley at 781 m elevation) and Chamrousse (1729 m), located on a topographic ridge, is almost 950 m. During this long persistent inversion, the tn and tx of the plain are respectively 5.5 and 6.5°C colder than those of the mountain. During the period, the weather did not remain fine, quite the contrary. Several, only slightly active, atmospheric depressions crossed the region bringing cloud and precipitation. Despite this, the inversion persisted, showing that confinement, associated with valley depth, is a sufficient rampart to keep the air cold (Largeron and Staquet, 2016a; Arduini *et al.*, 2020) and, as a collateral problem, for pollutants to accumulate (Largeron and Staquet, 2016b). This problem recurrently affects all Alpine valleys (Paci *et al.*, 2015).

4.5. Site typology

The typology of sites with respect to inversions (section 3.3.) does not clearly show large differences between classes. The differences appear through details. For example, the stations in the Massif Central, the Cévennes, and the Vosges feature in all three classes, while those in Normandy figure in two classes. However, it should be noted that the high mountain resorts (north of the Alps and Pyrenees) are consistently classified (class 1). This aspect refers to the complexity of the phenomenon of inversions which originate anywhere, even on the plains, as soon as the atmospheric conditions are favourable (Joly and Richard, 2003). The ascending hierarchical classification is apparently not able to account effectively for this diversity. The use of other computational algorithms (Joly and Langrognet, 2015) would have made it possible to overcome this limitation by proposing more robust classes.

Conclusion

The challenge of this work was twofold. Firstly, it was theoretical: to determine how the three characteristics of inversions (intensity, frequency, duration) are distributed in space. It was also practical: to identify the factors that can be used to statistically disaggregate the outputs of GCMs (CMIP type) or RCMs (CORDEX type) at fine scales. At the end of this study, the first challenge

has been met, at least in many respects. Several conclusions argue in this sense, even if they show that reality is far more complex than expected.

Topographic descriptors do not act in the same way on the three indicators of inversions. For example, elevation has no influence on the frequency of inversions but has a crucial effect on their intensity and duration. Other topographic variables (valley, hump, amplitude) have a decisive influence on all indicators. The shape of the estimate also shows that the topographic variables explain the spatial variation of the inversions according to different categorizations: linearly, polynomially for complex shapes, or logarithmically when the variations occur over short distances (distance to the nearest sea).

The type of inversion also plays an important role according to the way they are structured in space. In valley bottoms, persistent inversions and late night inversions (tn) last much longer than daily inversions (tx). Conversely, the more prominent the relief, the lower the value of the characters of the tn-inversions, the reverse being observed for the tx-inversions. The prominence of relief thus plays a moderating role on the tn-inversions and tends to exaggerate the characters of the tx-inversions. Similarly, the influence of the distance to the sea is systematically reversed between night and daytime inversions. The sign of the correlation is systematically reversed between nocturnal and diurnal inversions.

Regression analysis, mapping, and classification reveal that the spatial variation of the three indicators of inversions occurs at two nested scales. At a fine scale, the characters of the inversions vary according to the local topographic features: valleys make for more intense and more frequent inversions whereas inversions are much weaker and rarer on ridges. This is particularly the case in complex mountain massifs, the Alps for example, where a multitude of small, elongated, contrasting sectors with alternating high and low frequencies are juxtaposed. Nationwide, there are also far larger areas conducive to inversions and others that are much less so. The effects of these two mechanisms are compounded with the result that mapping reveals a complex situation where it is seldom possible to find simple patterns.

The major point is that the variations of inversions in space are inseparable from their variations in time. The second objective we had set ourselves is not fully achieved. Forecasting the occurrence of an inversion and its intensity in a given place is not a straightforward matter. Successful forecasting would involve integrating the configuration of the place, in particular the topography which may or may not be conducive to inversions. However, sites where inversions are frequent and intense, the bottom of deep valleys, among others, do not invariably see inversions form; in addition to topography, weather conditions also influence the occurrence of inversions, as we saw in the study of temporal variations of inversions (Joly and Richard, 2022). Thus, forecasting the appearance of an inversion at XY on day+1 requires the use of weather forecasts that establish conducive and inconducive meteorological conditions for the next day for any point in the territory on a medium scale. With the use of information from topography, it is, however, possible to refine these spatio-temporal patterns by downscaling the forecast to fine scales.

Acknowledgements: We are grateful to Météo-France for making the data available under the agreement signed with the University of Burgundy.

References

Anquetin S., Guilbaud C., Chollet J.-P., 1998. The formation and destruction of inversion layers within a deep valley. *J. Appl. Meteor*. 37: 1547-1560.

Arduini G. Chemel C., Staquet C., 2020. Local and non- local controls on a persistent cold- air pool in the Arve River Valley. *Quarterly Journal of the Royal Meteorological Society*, 146: 2497-2521. https://doi.org/10.1002/qj.3776

Barry R. G., 2008. *Mountain Weather and Climate*. 3rd ed. Cambridge University Press, 506 p.

Burns P. and Chemel C., 2015. Interactions between downslope flows and a developing cold-air pool. *Boundary-Layer Meteorology*, 154: 57-80.

Busch N., Ebel U., Kraus H., Schaller E., 1982; The structure of the subpolar inversion-capped atmospheric boundary layer (ABL). *Arch. Met. Geoph. Biokl*., Ser. A, 31: 1-18.

Daly C., Conklin D. R., Unsworth M. H., 2010. Local atmospheric decoupling in complex topography alters climate change impacts. *Int. J. Clim*., 30(22): 1857-1864; https//doi: 10.1002/joc.2007

Dorninger M., Whiteman C. D., Bica B., Eisenbach S., Pospichal B., Steinacker R., 2011. Meteorological events

affecting cold-air pools in a small basin. *Journal Appl. Meteorol. Climatol*., 50: 2223-2234.

Ehret U., Zehe E., Wulfmeyer V., Warrach-Sagi K., Liebert J., 2012. HESS Opinions 'Should we apply bias correction to global and regional climate model data?'. *Hydrol. Earth Syst. Sci. Discuss*., 9: 5355-5387. https//doi:10.5194/hessd-9-5355-2012

Enayati M., Bozorg-Haddad O., Bazrafshan J., Hejabi S., Chu X., 2021. Bias correction capabilities of quantile mapping methods for rainfall and temperature variables. *Journal of Water and Climate Change*, 12(2): 401-4019.

Fallot J.-M., 2012. Influence de la topographie et des accumulations d'air froid sur les températures moyennes mensuelles et annuelles en Suisse. In Bigot S. et Rome S. (eds.), 25ème colloque de l'Association Internationale de Climatologie (AIC): 273-278.

Fernando H. J. S., Verhoef B., Di Sabatino S., Leo L. S., Park S., 2013. The Phoenix Evening Transition Flow Experiment TRANSFLEX. *Boundary-Layer Meteorolog.*, 147: 443-468. https://doi.org/10.1007/s10546-012-9795-5

Gaillardet J., Braud I., Hankard F., Anquetin S., Bour O., Dorfliger N. *et al.*, 2018. OZCAR: The French Network of Critical Zone Observatories. *Vadose Zone J*., 17: 180067. doi:10.2136/vzj2018.04.006

Garratt J. R., Hess G. D., Physick W. L., Bougeault P., 1996. The atmospheric boundary layer – advances in knowledge and application. *Boundary-Layer Meteorol.*, 78: 9-37. doi.org/10.1007/BF00122485

Giorgi F., Marinucci M. R., Bates G. T., 1993. Development of a Second Generation Regional Climate Model (RegCM2). Part 1: Boundary-layer and radiative transfer processes. *Monthly Weather Review*, 121: 2794-2813.

Helmis C. G., Papadopoulos K. H., 1996. Some aspects of the variation with time of katabatic flows over a simple slope. *Quarterly Journal of the Royal Meteorological Society*, 122: 595-610. https://doi.org/10.1002/qj.49712253103

Joly D., Berger A., Buoncristiani J.F., Champagne O., Pergaud J., Richard Y., Soare P., Pohl B., 2018. Geomatic downscaling of temperatures in the Mont-Blanc massif. *International Journal of Climatology*, 38 (4): 1846-1863, DOI: 10.1002/joc.5300

Joly D., Bois B., Zaksek K., 2012. Rank-ordering of topographic variables correlated with temperature. *Atmospheric and Climate Science*, 2(2): 139-147. http://dx.doi.org/10.4236/acs.2012.22015

Joly D., Brossard T., Cardot H., Cavailhès J., Hilal M., Wavresky P., 2010. Les types de climats en France, une construction spatiale (Types of climate in continental France, a spatial construction). *Cybergeo: European Journal of Geography*, 501. http://cybergeo.revues.org/index23155.html

Joly D., Brossard T., Cardot H., Cavailhès J., Hilal M., Wavresky P., 2011. Temperature interpolation by local information; the example of France. *International Journal of Climatology*, 31(14): 2141-2153.

Joly D., Langrognet F., 2015. Pertinence du découpage spatial produit par deux méthodes de classification (CHA et MIXMOD) ; application aux climats français. Cybergeo: *European Journal of Geography* [En ligne], Cartographie, Imagerie, SIG, document 761, DOI: 10.4000/cybergeo.27414.

Joly D., Richard Y., 2018. Topographic descriptors and thermal inversions amid the plateaus and mountains of the Jura (France). *Climatologie* [Online], updated on: 02/10/2019. lodel.irevues.inist.fr/climatologie/index.php?id=1335.

Joly D., Richard Y., 2022. Temperature inversions in France – Part A: time variations. *Climatologie*, 19, 4.

Largeron Y., Staquet C., 2016a. The atmospheric boundary layer during wintertime persistent inversions in the Grenoble valleys. *Front. Earth Sci*., 4(87). https//doi: 10.3389/feart.2016.00070

Largeron Y., Staquet C., 2016b. Persistent inversion dynamics and wintertime PM 10 air pollution in Alpine valleys. *Atmos. Environ.*, 135: 92-108. https//doi: 10.1016/j.atmosenv.2016.03.045

Liang S., Qin J., 2008. Data assimilation methods for land surface variable estimation. In: Liang S. (eds) *Advances in Land Remote Sensing*. Springer, Dordrecht. https://doi.org/10.1007/978-1-4020-6450-0_12.

Lundquist J. D., Pepin N. and Rochford C., 2008. Automated algorithm for mapping regions of cold- air pooling in complex terrain. *Journal Geophysical Research*, 113: D22107.

Mahrt L., Richardson S., Seaman N., Stauffer D., 2010. Non-stationary drainage flows and motions in the cold pool. *Tellus*, 62: 698-705. https//doi.org/10.1111/j.1600-0870.2010.00473.x

Paci A., Staquet C., *et al.*, 2015. *The Passy-2015 field experiment: An overview of the campaign and preliminary results*. Proc. of the 33rd International Conference on Alpine Meteorology, Innsbruck, Austria.

Papadopoulos K. H., Helmis C. G., 1999. Evening and morning transition of katabatic flows. *Boundary-Layer Meteorology*, 92: 195-227. https://doi.org/10.1023/A:1002070526425

Planchon O., Cautenet S., 1997. Rainfall and sea- breeze circulation over South- Western France. *Int. Journal Climatol.*, 17(5): 535-549. https//doi.org/10.1002/(SICI)1097-0088(199704)17:5<535::AID-JOC150>3.0.CO;2-L

TongY., Gao X., Han Z., Xu Y., Giorgi F., 2021. Climate Dynamics, 57: 1425-1443. https://doi.org/10.1007/s00382-020-05447-4

Citation of article : Joly D. et Richard Y., 2022. Temperature inversions in France – Part B: spatial variations. *Climatologie*, 19, 5.